Synthesis and Structural Characterization of MWW Type Zeolite ITQ-1, the Pure Silica Analog of MCM-22 and SSZ-25

Miguel A. Camblor,* Avelino Corma, and María-José Díaz-Cabañas

Instituto de Tecnología Química, CSIC-UPV, Universidad Politécnica de Valencia, Avda. Los Naranjos s/n, 46071 Valencia, Spain

Christian Baerlocher*

Laboratory of Crystallography, ETH, CH-8092 Zurich, Switzerland

Received: July 16, 1997; In Final Form: October 8, 1997[⊗]

The synthesis of pure silica MWW type zeolite ITQ-1 using trimethyladamantammonium ($TMAda^+$) is described. The reproducibility of the synthesis, as well as the quality of the materials obtained, is greatly improved if the synthesis is assisted by hexamethyleneimine (HMI) as a second organic additive. As $TMAda^+$ is too large to fit into the sinusoidal 10 MR channel (i.e., the channel delimited by a ring of 10 tetrahedra), the stabilization of this channel seems to require the presence of additional organic moieties. In the absence of HMI, these probably come from either the partial degradation of $TMAda^+$ or from organics adsorbed on the PTFE liners in previous syntheses. The use of $TMAda^+$ and HMI and Na^+ cations allows a fast and highly reproducible synthesis of pure silica ITQ-1. The material obtained shows an improved crystallinity in both the as-made and the calcined form. The structure of calcined ITQ-1 has been refined in space group *P*6/*mmm* ($a = 14.2081(1)$ Å, $c = 24.945(2)$ Å, $R_{exp} = 0.103$, $R_{wp} = 0.159$, $R_f = 0.065$), using synchrotron powder diffraction data, and the topology previously proposed for the aluminosilicate MCM-22 zeolite has been confirmed. Comparison of the highly resolved ^{29}Si MAS NMR spectra of as-made and calcined ITQ-1 show that in the as-made form there is a high concentration of Si−OH defect groups, which are annealed upon calcination and which arise from a lack of connectivity between specific Si sites.

Introduction

MCM-22 is an aluminosilicate zeolite for which an interesting and unusual framework structure, containing two independent systems of 10 MR channels and a large supercage, has been proposed.[1] Such a structure should give MCM-22 interesting shape selectivity properties in catalysis. However, the Rietveld refinement of MCM-22 in the space group *P*6/*mmm* yielded very high residuals and the symmetry imposed some Si−O−Si angles of 180°, considered unlikely to exist in reality. Reducing the space group symmetry to *Cmmm* removed these symmetry constraints, but the Rietveld refinement was then unsatisfactory.[1]

The synthesis of the pure silica analogue of MCM-22, ITQ-1, was reported recently.[2] In an effort to solve the reproducibility problems in this synthesis, new methods to prepare materials with improved crystallinity compared to previously reported materials of the same family have been developed. The higher quality of the powder diffraction data allowed a structure analysis using the Rietveld method to be undertaken. The result of these investigations into the synthesis optimization and the structural characterization of ITQ-1 are the subject of the paper.

Experimental Section

Synthesis. A summary of synthesis conditions and results is given in Table 1. For the synthesis of ITQ-1 using only *N*,*N*,*N*-trimethyl-1-adamantammonium hydroxide ($TMAda^+ OH^-$) as a structure-directing agent, no alkali cations were used.[2] TMAdaOH was prepared by anion exchange of the iodide, which was obtained by reaction of 1-adamantylamine with an excess of methyl iodide at room temperature. An example of the procedure for the synthesis of ITQ-1 is as follows: 1.125 g of silica (Aerosil 200, Degussa) was added under stirring to a solution made with 11.141 g of a 0.42 M solution of TMAdaOH and 4.733 g of deionized water. The mixture was then transferred to a 60 mL PTFE lined stainless steel autoclave and heated for 17 days at 423 K while being rotated at 60 rpm. After filtering, the white solid was washed with deionized water until the pH was ca. 9. When amines or NaCl was used in the synthesis, it was added to the TMAdaOH solution, and the mixture was homogenized before addition of the silica. The synthesized solids referred to as ITQ-1 in Table 1 are probably a layered precursor of the three-dimensional, fully connected ITQ-1, which was obtained by calcination in air at 580 °C for 3 h. The solids termed L1 and L2 in Table 1 are unknown products of layered nature and shall not be confused with the layered precursor of ITQ-1.

Reference MCM-22 (Si/Al = 19), SSZ-25 (Si/Al = 28), and MCM-49 (Si/Al = 10) samples were prepared according to the procedures reported in refs 3, 4, and 5, respectively.

Characterization. Conventional powder XRD data were recorded on a Philips 1060 diffractometer (Cu Kα radiation, graphite monochromator) provided with a variable divergence slit and working in the fixed irradiated area mode. C, H, and N contents were determined with a Carlo Erba 1106 elemental organic analyzer, and the results are presented in Table 2.

* M. A. Camblor: macamblo@itq.upv.es. Fax: 34-6-3877809. Ch. Baerlocher: ch.baerlocher@kristall.erdw.ethz.ch. Fax: 41-1-632 1133.

⊗ Abstract published in *Advance ACS Abstracts,* December 15, 1997.

S1089-5647(97)02319-5 CCC: $15.00
Published on Web 01/01/1998

TABLE 1: Summary of Synthesis Conditions and Results

run	gel composition	T (°C)	t (days)	product
MD7	SiO_2:0.26TMAdaOH:43H_2O	150	9	L1
			14	ITQ-1
83MC	SiO_2:0.25TMAdaOH:44H_2O	150	17	ITQ-1
MD16	SiO_2:0.25TMAdaOH:43H_2O	150	14	L1+ITQ-1
			21	SSZ-31
MD32	SiO_2:0.26TMAdaOH:44H_2O	150	15	L1
			21	SSZ-31+ITQ-1
MD42	SiO_2:0.26TMAdaOH:44H_2O	150	15	SSZ-31+SSZ-23
			19	SSZ-31+SSZ-23
MD148	SiO_2:0.25TMAdaOH:44H_2O	150	15	L1
			21	L1
MD55	SiO_2:0.25TMAdaOH:44H_2O	140	14	L1
			21	L1
MD89	SiO_2:0.25TMAdaOH:44H_2O	165	9	SSZ-31
			14	SSZ-31+TRID
			21	TRID
MD61	SiO_2:0.32TMAdaOH:44H_2O	150	3	amorphous
			7	L1+SSZ-24
			14	SSZ-24+L1+SSZ-23
MD67	SiO_2:0.28TMAdaOH:44H_2O	150	7	L1
			14	L1+ITQ-1
			21	SSZ-31+L1
MD20	SiO_2:0.25TMAdaOH:0.31HMI:44H_2O	150	9	ITQ-1
			14	ITQ-1
			28	ITQ-1+NON
MD45	SiO_2:0.25TMAdaOH:0.31HMI:44H_2O	150	3	ITQ-1
			5	ITQ-1
MD44	SiO_2:0.25TMAdaOH:0.31HMI:44H_2O	150	7	ITQ-1
			9	ITQ-1
			14	ITQ-1
			28	ITQ-1+NON
			45	NON
MD56	SiO_2:0.25TMAdaOH:0.31HMI:44H_2O	150	3	ITQ-1
MD71	SiO_2:0.25TMAdaOH:0.31HMI:44H_2O	150	7	ITQ-1
MD49	SiO_2:0.25TMAdaOH:0.06HMI:44H_2O	150	2	amorphous
			3	amorphous
			7	L1
			14	SSZ-31
			17	ITQ-1+SSZ-31
MD96	SiO_2:0.25TMAdaOH:0.40HMI:44H_2O	150	3	ITQ-1
MD78	SiO_2:0.25TMAdaOH:0.31HMI:0.15NaCl:44H_2O	150	5	ITQ-1
			7	ITQ-1
			14	ITQ-1
MD84	SiO_2:0.25TMAdaOH:0.31HMI:0.20NaCl:44H_2O	150	5	ITQ-1
			7	ITQ-1[a]
			14	ITQ-1
MD88	SiO_2:0.25TMAdaOH:0.31HMI:0.30NaCl:44H_2O	150	5	ITQ-1
			7	ITQ-1
			14	L2+SSZ-31
MD91&97	SiO_2:0.25TMAdaOH:0.31HMI:0.20NaCl:44H_2O	150	7	ITQ-1
MD4	SiO_2:0.15TMAdaOH:0.12KOH:33H_2O	150	6	SSZ-24
			9	SSZ-24+SSZ-31
MD25	SiO_2:0.15TMAdaOH:0.12KOH:33H_2O	150	7	SSZ-24
MD170	SiO_2:0.25TMAdaOH:0.20NaCl:44H_2O	150	5	amorphous+SSZ-31
MD65	SiO_2:0.25TMAdaOH:0.31DPA:44H_2O	150	3	amorphous
			7	L1+ITQ-1
			13	ITQ-1
MD154	SiO_2:0.25TMAdaOH:0.31DBA:44H_2O	150	7	amorphous
			14	amorphous+SSZ-31

[a] Sample used in the Rietveld refinement. L1 and L2 are layered phases of unknown structure. HMI is hexamethyleneimine, DPA is dipropylamine, and DBA is diisobutylamine

Thermogravimetric analyses were performed on a NETZSCH STA 409 EP thermal analyzer in the 293−1173 K range with ca. 0.0200 g of sample, a heating rate of 10 K/min, and an air flow of 6 L/h. NMR spectra were recorded on a Varian VXR 400SWB spectrometer. The ^{29}Si MAS NMR spectra were recorded with a spinning rate of 5.5 kHz at a ^{29}Si frequency of 79.459 MHz with a 55.4° pulse length of 4.0 μs and a recycle delay of 60 s. The ^{1}H→^{13}C CPMAS NMR spectra were acquired with a spinning rate of 4 kHz at a ^{13}C frequency of 100.579 MHz with a 90° pulse length of 7.5 μs, a contact time of 5000 μs, and a recycle delay of 2 s. Both ^{29}Si and ^{13}C chemical shifts are reported relative to TMS.

X-ray Data Collection. For the structure analysis, synchrotron powder data were collected for ITQ-1 on the Swiss Norwegian Beamline at the ESRF in Grenoble. Table 3 lists the experimental details. The high angle part of the pattern (from 20° 2θ onward) was measured at least twice as long (30−40 s/step) as the lower angle region. After normalization for constant monitor counts, the background was estimated by hand and subtracted.

TABLE 2: Chemical Composition of As-Made Pure Silica ITQ-1 Samples Synthesized in Different Conditions

run	additives[a]	%N	%C	%H	C/N	TG[b]	%Na
MD7B		0.935	10.843	1.879	13.5	15.64	
83MC3		1.318	14.751	2.381	13.1	19.49	
MD20A	HMI	1.796	15.492	2.646	10.1	23.47	
MD45A	HMI	1.722	15.098	2.662	10.2	23.05	
MD44A	HMI	1.832	15.407	2.708	9.8	23.79	
MD56	HMI	1.398	11.644	2.122	9.7	16.79	
MD96	HMI	1.825	16.004	2.822	10.2	25.22	
MD78A	HMI+Na	1.602	13.041	2.238	9.5		0.03
MD78B		1.668	13.739	2.443	9.6	19.54	0.01
MD78C		1.664	13.663	2.418	9.6		
MD84A	HMI+Na	2.150	16.248	2.784	8.8		0.05
MD84B[c]		1.973	16.203	2.781	9.6	24.98	0.04
MD88B	HMI+Na	1.880	15.714	2.735	9.7	23.22	0.07
MD91	HMI+Na	1.824	15.338	2.641	9.8	22.44	0.04
MD97	HMI+Na	1.878	15.540	2.727	9.7	24.46	
MD65C	DPA	1.551	15.054	2.636	11.3	23.05	

[a] In addition to $TMAda^+$. [b] Weight loss by thermogravimetric analysis to 1173 K. [c] Sample used in the Rietveld refinement.

TABLE 3: Experimental and Crystallographic Data for ITQ-1, the Pure Silica Polymorph of MCM-22

data collection	
synchrotron facility	ESRF
beamline (capillary mode with Si 111 analyzer crystal)	SNBL
capillary, size (mm)	1
wavelength (Å)	1.10014
2θ range (°2θ)	2.2−50.0
step size (°2θ)	0.01
unit cell	
unit cell formula	$Si_{72}O_{144}$
space group	*P*6/*mmm*
a (Å)	14.2081(1)
c (Å)	24.945(2)
refinement	
standard peak for peak shape function (*hkl*, °2θ)	1 0 2, 7.20
step size for calculation of esd's (°2θ)	0.06
smallest fwhm at beginning of pattern (*hkl*, °2θ)	1 0 0, 0.028
largest fwhm at beginning of pattern (*hkl*, °2θ)	0 0 1, 0.14
peak range (number of fwhm)	20
number of observations	4749
number of contributing reflections	422
number of geometric restraints	58
number of structural parameters	37
number of profile parameters	10
R_{exp}	0.103
R_{wp}	0.159
R_f	0.065

Results and Discussion

Synthesis. When $TMAda^+$ is used as the only organic structure-directing agent in the synthesis of pure silica phases, the product of the synthesis strongly depends on the presence of alkali cations: Gittleman et al.[6] reported very recently that in the presence of K^+ SSZ-24 crystallizes, while the use of Na^+ yields SSZ-31 and other phases are obtained with Rb^+ and Cs^+. Similarly, under certain conditions for Al-containing mixtures, Zones et al.[7] reported that the alkali cation (Na^+ or K^+) content can determine the nature of the phase obtained (SSZ-13 or SSZ-23). Contrarily to previous reports that no crystallization takes place in the absence of alkali cations,[6] with our synthesis conditions we were able to synthesize pure silica ITQ-1 in the absence of alkali cations.[8] This is the high-silica analogue of zeolites PSH-3,[9] MCM-22,[10] SSZ-25[4], and ERB-1.[11] It should be noted that in the absence of $TMAda^+$ the hexamethyleneimine (HMI)-mediated synthesis of pure silica MCM-22, ERB-1, or PSH-3 has never been reported. Moreover, the Si/Al ratio that can be obtained by direct unseeded synthesis of MCM-22 appears to present a rather low upper limit, and a severe decrease of the crystallinity was found for final materials with Si/Al > 50[3] (with a concomitant uncertainty in the actual Si/Al ratio of the crystalline fraction of the product). On the other hand, the synthesis of SSZ-25 using only $TMAda^+$ in the presence of alkali cations suffers from the same drawback with respect to the narrow range of Si/Al attainable by direct synthesis (15 to 50, as claimed in ref 4), and, as remarked by Chan et al., "aluminium does seem to be required for its synthesis".[12]

The crystallization of ITQ-1 under these conditions ($TMAda^+$ as the only organic structure-directing agent) is preceded by the crystallization of a layered silicate of unknown structure (termed L1 in Table 1). Although we were able to obtain pure ITQ-1 twice under these conditions, the synthesis is long and difficult to reproduce (Table 1). Typically, zeolites SSZ-31 and, to a lesser extent, SSZ-23, also appear, sometimes without detectable cocrystallization of ITQ-1. Zones et al.[7] pointed out that there is considerable overlapping of the crystallization fields of SSZ-23, SSZ-24, and SSZ-13 from $TMAda^+$-containing mixtures. Given this very low specificity of $TMAda^+$ as a structure-directing agent, we tried to find better crystallization conditions for ITQ-1 by changing several parameters but had no success: decreasing and increasing the crystallization temperature favored the layered phase L1 and zeolite SSZ-31 (with tridymite appearing at longer time), respectively, while too high a $TMAda^+$ content changed the crystallization to SSZ-24 and SSZ-23 (Table 1).

However, when HMI, the organic structure-directing agent of zeolite MCM-22, is used together with $TMAda^+$, the crystallization time is considerably shortened (3 days compared to 14−17) and, more importantly, the synthesis becomes highly reproducible (Table 1).[13] For HMI/SiO_2 ratios in the range 0.31−0.40, none of the phases that appear in the absence of HMI have been detected, and only after very long crystallization times does nonasil start to grow at the expense of ITQ-1. The amount of HMI necessary to observe its beneficial effect is not extremely critical. For HMI/Si ratios between 0.31 and 0.40, the crystallization is complete in 3 days. Moreover, for HMI/SiO_2 ratios as low as 0.06 the crystallization of ITQ-1 occurs even after SSZ-31 started to crystallize. The chemical composition of ITQ-1 samples synthesized under several sets of conditions are reported in Table 2. The C/N ratio in the absence of HMI is close to the value of $TMAda^+$ (13), while in the presence of HMI large deviations are found (C/N = 8.8−10.2, typically ca. 9.7), suggesting that nearly equal amounts of $TMAda^+$ and HMI are incorporated in the final material. The total amount of organic material is generally much larger when the synthesis is carried out in the presence of HMI. The

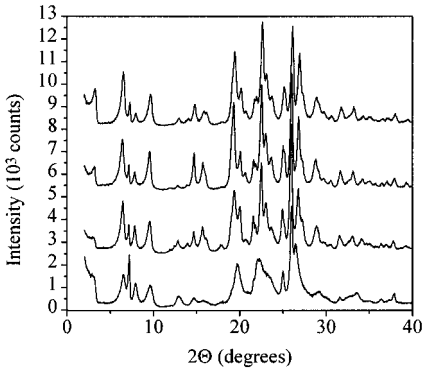

Figure 1. Powder X-ray diffraction patterns of as-made (from bottom to top) MCM-22, SSZ-25, and pure silica ITQ-1 synthesized using $TMAda^+$ alone and $TMAda^+$ and HMI.

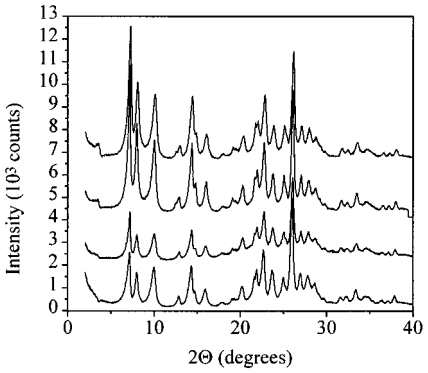

Figure 2. Powder X-ray diffraction patterns of calcined (from bottom to top) MCM-22, SSZ-25, and pure silica ITQ-1 synthesized using $TMAda^+$ alone and $TMAda^+$ and HMI.

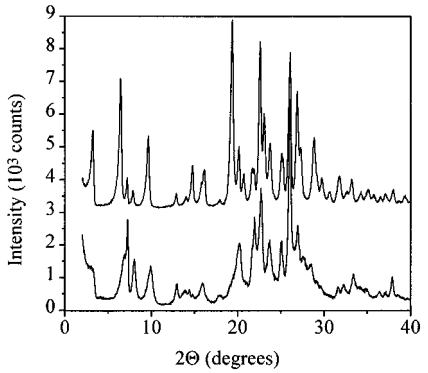

Figure 3. Powder X-ray diffraction patterns of as-made (from bottom to top) MCM-49 and pure silica ITQ-1 synthesized using $TMAda^+$, HMI, and Na^+.

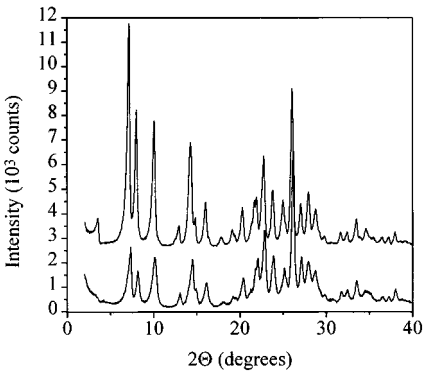

Figure 4. Powder X-ray diffraction patterns of calcined (from bottom to top) MCM-49 and pure silica ITQ-1 synthesized using $TMAda^+$, HMI, and Na^+.

variations in total organic content observed in Table 2 for samples synthesized under similar conditions are not unexpected given the layered nature of the as-made precursor and the fact that most of the organic species must reside in the interlayer region.

The powder XRD pattern of ITQ-1, whether synthesized from $TMAda^+$ alone or with HMI added, is better resolved than those of MCM-22 and SSZ-25 and shows an improved crystallinity. This is true for the as-made precursor (Figure 1) and becomes even more apparent in the final zeolite obtained by calcination (Figure 2).

It is also remarkable that the addition of Na^+ cations, which lead to zeolite SSZ-31 in the absence of HMI (see Table 1), is not detrimental to the synthesis of ITQ-1 with $TMAda^+$ and HMI, at least for Na^+/SiO_2 ratios up to 0.3 and not too long crystallization times. For $Na^+/SiO_2 = 0.3$ SSZ-31 and a second layered phase (L2) appear only after a long crystallization time (14 days, Table 1). Moreover, it has been reported that for MCM-22 Na^+/HMI molar ratios greater than 0.5 lead to zeolite MCM-49.[14] This zeolite is claimed to have the fully connected 3-D framework in its as-synthesized form, whereas for MCM-22 this is only obtained upon calcination. However, in the synthesis of pure silica ITQ-1, addition of Na^+ to a reaction mixture containing $TMAda^+$ and HMI does not result in any noticeable change in the peak positions of the XRD powder diffraction pattern, which still corresponds to the layered precursor (Figure 3). It is, nevertheless, remarkable that under these conditions a further improvement in crystallinity is found for both the calcined material (Figure 4) and, especially, the as-made one (Figure 3). Table 2 shows that the Na^+ content of the samples synthesized in the presence of this cation is always very small. In conclusion, addition of HMI to the crystallization mixture of pure silica ITQ-1 allows a shorter and more reproducible synthesis and widens its crystallization field (at least with respect to its tolerance to Na^+).

The ^{13}C CPMAS NMR spectra of ITQ-1 synthesized with $TMAda^+$ alone and with $TMAda^+$ and HMI are given in Figure 5, together with the ^{13}C NMR spectrum of $TMAda^+I^-$, HMI, and HMI:HCl in $CDCl_3$ solution. These spectra suggest three relevant facts: (1) $TMAda^+$ is always found intact inside the as-made ITQ-1 samples; (2) HMI is also found when used in the reaction mixture (although, because of severe overlapping of the expected resonances of HMI with those of $TMAda^+$, it is unclear whether it is protonated or not); and (3) when no HMI is added to the synthesis gel, the sample contains additional organic moieties. We were unable to determine the nature of this organic species (although they are most likely amines) which were not detected previously by Bloch decay ^{13}C MAS NMR[2] and speculate that they probably come from either partial decomposition of $TMAda^+$ or organic products adsorbed on the PTFE liners from previous syntheses. The third point above might explain the poor reproducibility of the synthesis of ITQ-1 using $TMAda^+$ and also the role of HMI in the synthesis. It is clear that, because of its size (cross section of ca. 6.6−7 Å), $TMAda^+$ cannot be occluded in the sinusoidal medium 10 MR pores of the structural model proposed for MCM-22. However, it has shown a tendency to direct the syntheses toward zeolites with 12 MR pores (SSZ-24,[15] VPI-8[16]) or cages (SSZ-13[7]). Accepting that MCM-22, SSZ-25, and ITQ-1 are isomorphous and given that no alkali cations are necessary in the synthesis of pure silica ITQ-1, one can wonder about what fills the sinusoidal 10 MR channels of ITQ-1 when only $TMAda^+$ is used as the structure-directing agent. As water is not a good candidate as a pore filler in a pure silica phase (even in the

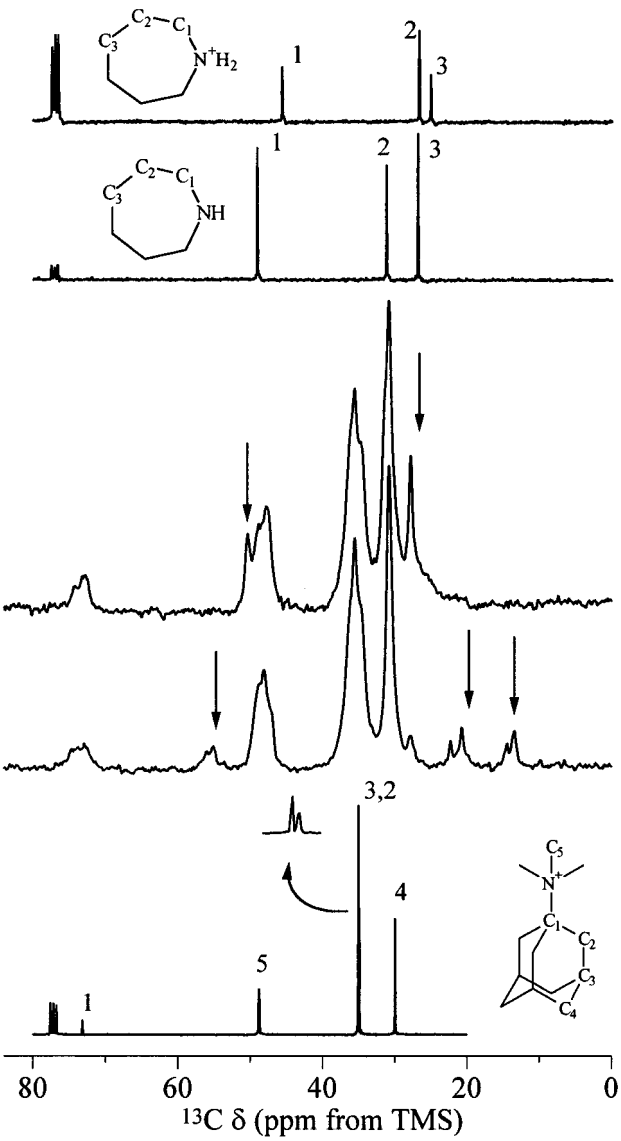

Figure 5. ^{13}C NMR spectra of (bottom to top): TMAdaI; ITQ-1 synthesized using $TMAda^+$ alone; ITQ-1 synthesized using $TMAda^+$ and HMI; HMI; and HMI:HCl. The spectra of the organics are Bloch decay ^{13}C NMR in $CDCl_3$ solution, while those of ITQ-1 are ^{13}C CPMAS NMR of the solids. The arrows denote resonances that are not attributable to $TMAda^+$. The figures near each peak are the assignments to the corresponding C in each drawing.

presence of Si−OH defects), the above results support our very recently proposed hypothesis on the beneficial effect of HMI in the TMAda-mediated synthesis of ITQ-1.[2] The stabilization of two types of void spaces could be best accomplished by the cooperative use of the imine (to stabilize the 10 MR channel) and 1-$TMAda^+$ (to stabilize the 12 MR cage). Moreover, in the absence of HMI (or other suitable organic additive, see below) crystallization would be facilitated only through "accidentally present" organics of suitable size to fill the sinusoidal 10 MR, such as organic fragments coming from the partial decomposition of a fraction of the $TMAda^+$ or from the PTFE liners. This would explain the longer crystallization time needed in the absence of HMI (or other additives) and, more importantly, the poor reproducibility of such crystallizations. The fact that, in the absence of HMI, the C/N ratio does not deviate significantly from the value of $TMAda^+$ (Table 2) suggests that most of the organic species are actually $TMAda^+$ occluded in the interlayer region and that very little additional organic

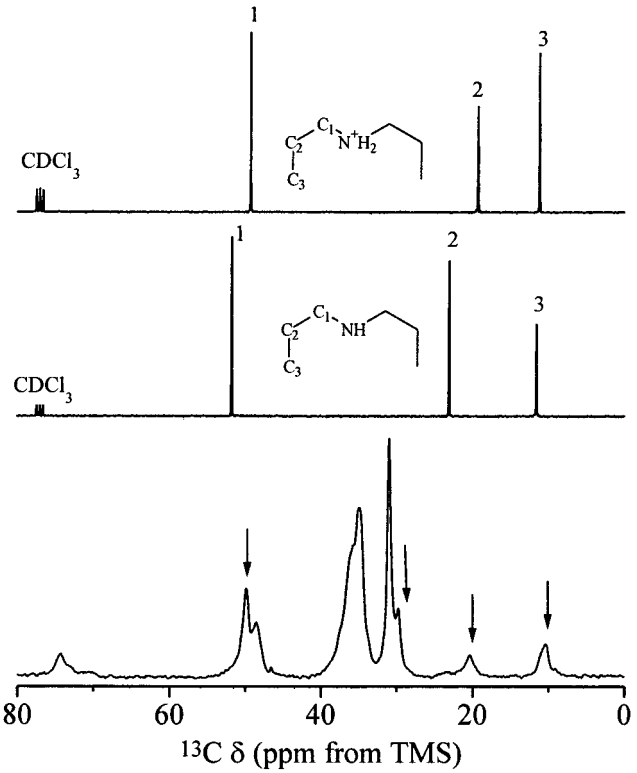

Figure 6. ^{13}C NMR spectra of (bottom to top): ITQ-1 synthesized using $TMAda^+$ and DPA; DPA; and DPA:HCl. The spectra of the organics are Bloch decay ^{13}C NMR in $CDCl_3$ solution, while that of ITQ-1 is a ^{13}C CPMAS NMR of the solid. The arrows denote resonances that are not attributable to $TMAda^+$. The numbers near each peak are the assignments to the corresponding C in each drawing.

moieties (of unknown C/N ratio) are needed to help stabilize the intralayer sinusoidal channel.

To further clarify this point, we performed additional synthesis experiments in the presence of other additives: dipropylamine (DPA) and the bulkier diisobutylamine (DIBA). Being secondary amines, both of them will generate a similar pH effect on the reaction mixture as HMI, while DPA would be more suitable than DIBA as a pore filler of the sinusoidal 10 MR channels. Only with DPA did the synthesis yield ITQ-1 (Table 1), the C/N ratio (11.3, Table 2) suggesting that $TMAda^+$ and DPA are incorporated in the material in a ca. 3:1 ratio. The presence of both organics in ITQ-1 is confirmed by ^{13}C CPMAS NMR spectroscopy (Figure 6). This supports the view of a "cooperative structure-directing effect" of $TMAda^+$ and HMI or DPA, as these secondary amines help in the crystallization but are not specific templating agents. Thus, the role of DPA and HMI appears to be a stabilization effect by pore filling of the medium sinusoidal pores. However, an additional effect on the "gel chemistry" cannot be completely ruled out.

Structure Refinement. The synchrotron data clearly showed anisotropic line broadening (Figure 7). The 00*l* reflections were the broadest (starting with a full width at half-maximum (fwhm) of 0.14° 2θ for the 002 reflection), and the *hk*0 reflections the sharpest (fwhm of only 0.028° 2θ for the 100 reflection). This anisotropic line broadening was attributed to a crystal size effect using the following reasoning. As a result of the way the crystallites are thought to be formed during calcination of a layered precursor, the individual crystallites are not very well ordered in the *c*-direction. Consequently, the coherence length along *c* is much shorter than along the other directions. Using this interpretation, the fwhm for each reflection was calculated assuming a rotation ellipsoid for the crystal shape, with a

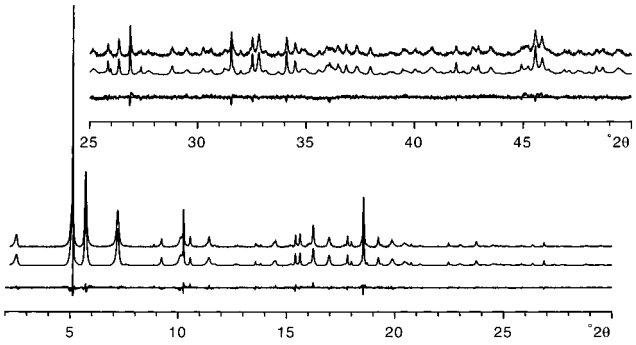

Figure 7. Observed (top), calculated (middle), and difference (bottom) plots for the Rietveld refinement of ITQ-1. The second half of the pattern has been scaled up by a factor of 8 to show more detail.

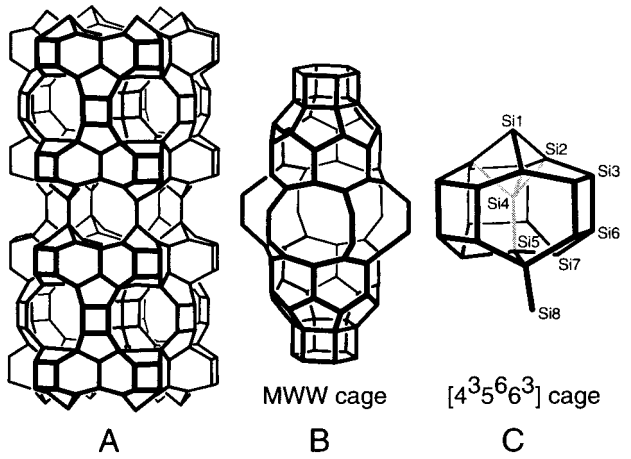

Figure 8. Skeletal drawings of the framework structure of ITQ-1 (MWW structure type): (A) the complete framework showing two double layers joined by single Si−O−Si bridges, (B) the large MWW cage, and (C) the small cage ($[4^35^66^3]$ cage) with labels for the Si atoms. Oxygen atoms have been omitted for clarity.

dimension of the two axes of approximately 250 and 6500 Å, respectively. In the actual refinement the "fine-tuning" of the fwhm was performed by dividing the reflections into three classes according to their position in the reciprocal space and refining the half width in these classes using a linear correction function.

The refinement, using the XRS-82 package of programs,[17] was initiated in the space group *P*6/*mmm* with the atomic coordinates from Leonowicz et al.[1] After the line broadening had been successfully modeled, the refinement converged quickly to the *R*-values reported in Table 3. A difference Fourier map showed no peak larger than 0.8 e/Å,[3] with the largest peak located at 0 0 1/2, in the center of the hexagonal prism. Attempts to include those peaks that had reasonable distances to the framework atoms as oxygens resulted in zero occupancy at these positions. Around the oxygens located on the 3-fold axis (O1 (between two Si1 atoms) and O5 (between Si4 and Si5), see Figure 8), some residual electron density remained (approximately 0.3 e/Å^3), indicating that these oxygens probably do not lie exactly on the 3-fold axis (thereby avoiding a Si−O−Si angle of 180°). However modeling this electron density either by an anisotropic refinement of the temperature factors of the two oxygens or by placing the oxygens off the 3-fold axis with an occupancy factor of 1/3 did not result in any significant improvement of the *R*-values. Therefore, no attempt was made to reduce the symmetry to *Cmmm*, especially since there was no indication of peak splitting in the powder pattern. However, the refinement had to be constrained by

TABLE 4: Atom Coordinates of ITQ-1, the Pure Silica Polymorph of MCM-22, in Space Group *P*6/*mmm*

atom	multiplicity	site symmetry	*x*	*y*	*z*	$U \times 100$
Si(1)	4	3*m*	2/3	1/3	0.0633(3)	1.4(1)
Si(2)	12	*m*	0.4685	0.2342(2)	0.1356(3)	1.4(1)
Si(3)	12	*m*	0.3904(4)	0	0.1607(3)	1.4(1)
Si(4)	4	3*m*	2/3	1/3	0.2108(4)	1.4(1)
Si(5)	4	3*m*	2/3	1/3	0.3404(4)	1.4(1)
Si(6)	12	*m*	0.3895(4)	0	0.2872(3)	1.4(1)
Si(7)	12	*m*	0.4215	0.2108(2)	0.3470(2)	1.4(1)
Si(8)	12	*m*	0.2544	0.1272(2)	0.4407(2)	1.4(1)
O(1)	2	6-*m*2	2/3	1/3	0	1.9(2)
O(2)	12	*m*	0.5411	0.2705(3)	0.0822(4)	1.9(2)
O(3)	24	1	0.3942(5)	0.1048(4)	0.1348(3)	1.9(2)
O(4)	12	*m*	0.5453	0.2726(3)	0.1882(4)	1.9(2)
O(5)	4	3*m*	2/3	1/3	0.2755(4)	1.9(2)
O(6)	12	*m*	0.3763(9)	0	0.2239(3)	1.9(2)
O(7)	6	2*mm*	1/2	0	0.1449(7)	1.9(2)
O(8)	6	2*mm*	1/2	0	0.3021(7)	1.9(2)
O(9)	24	1	0.3945(6)	0.1063(5)	0.3116(3)	1.9(2)
O(10)	12	*m*	0.5469	0.2735(3)	0.3638(4)	1.9(2)
O(11)	12	*m*	0.3536	0.1768(4)	0.4014(4)	1.9(2)
O(12)	12	*m*	0.1835(6)	0	0.4300(5)	1.9(2)
O(13)	6	*mm*2	0.3017	0.1508(7)	0.5000	1.9(2)

[a] The esd of the last significant digit is given in parentheses.

TABLE 5: Si−O−Si Angles for ITQ-1

Si1−O1−Si1	180[a]	Si6−O8−Si6	153(2.0)
Si1−O2−Si2	141(0.7)	Si6−O9−Si7	165(0.9)
Si2−O3−Si3	140(0.8)	Si5−O10−Si7	143(1.3)
Si2−O4−Si4	146(0.9)	Si7−O11−Si8	160(0.8)
Si4−O5−Si5	180[a]	Si8−O12−Si8	159(1.7)
Si3−O6−Si6	166(1.6)	Si8−O13−Si8	137(0.2)
Si3−O7−Si3	152(1.9)		

[a] Fixed by symmetry.

distance and angle restraints. The restraints used were as follows:

Si−O distance	1.61(1) Å
O−Si−O angle	109.47(1.0)°
Si−O−Si angle	145(8)°

with a common weight factor of 2.0. The isotropic displacement factors were constrained to be equal for all Si and all O atoms, respectively. The final parameters are listed in Table 4. Because of the use of distance and angle restraints, the resulting Si−O distances and O−Si−O angles are quite acceptable. The Si−O distances range from 1.57 to 1.62 Å and the O−Si−O angles from 107.0° to 111.6°. The resulting Si−O−Si angles are all listed in Table 5. The final Rietveld plot is shown in Figure 7.

This refinement confirms that ITQ-1 has indeed the same framework topology as MCM-22.[1] The code MWW has been assigned to this topology by the Structure Commission of the International Zeolite Association (IZA-SC). Although the structure has been described previously,[1] a skeletal drawing showing only the Si atoms is given in Figure 8. On the left side is a polyhedral view of the topology, where only windows larger than six-membered rings are transparent. Two double layers are joined by single Si−O−Si bridges (Si1 atoms), to generate one of the two independent two-dimensional channel systems. The second 2-D channel system lies within the double layer. Both channel systems have 10-ring openings, but the first system (between the layers) also has side pockets with a 12-ring access. These side pockets are on both sides of the channel system and form a large cage (MWW cage), which is hidden in the center of Figure 8A, but is drawn separately in

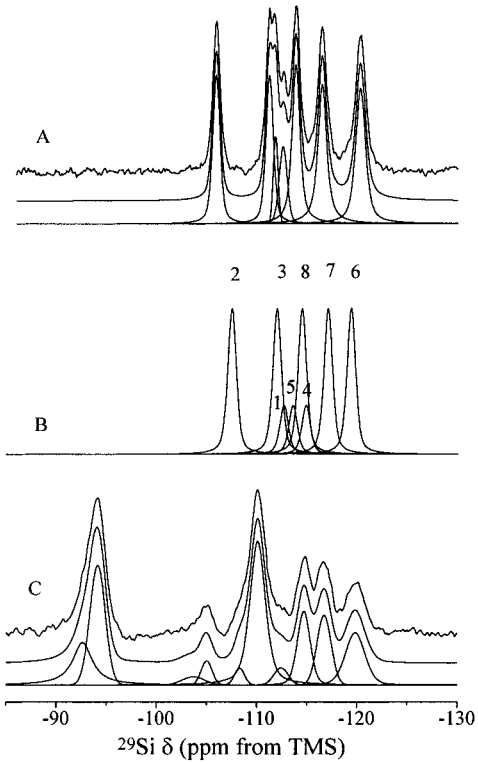

Figure 9. ^{29}Si MAS NMR spectra of calcined (A) and as-made (C) pure silica ITQ-1 synthesized in the presence of $TMAda^+$, HMI, and Na^+. In each case the upper trace is the experimental spectrum, the lower ones are the deconvoluted components, and the middle one is the simulated spectrum. Trace B is a simulation of the spectrum of calcined ITQ-1 calculated by using the Si−O−Si angles refined in this work and the equation of Thomas et al.[18]

Figure 8B. The double layers themselves can be viewed as a layer built from the small cages ($[4^35^66^3]$ cage) shown in Figure 8C, joined by double 6-rings. To build one such layer, the small cages are joined together via the three 4-rings. Six of these fused $[4^35^66^3]$ cages form part of the wall of the side pockets. Inside the small cage there is a further tetrahedral atom (Si4), which in Figure 8C is drawn in gray for clarity. However, there is nothing wrong with this tetrahedral atom. The fact that it is "inside" a cage is only the result of the way the structure has been described here. One could also describe the small cage (and hence the framework) as being built up from three $[4^15^26^2]$ cages which share six-membered rings. For easy reference in the discussion of the next section, the labels for the Si atoms are also included in Figure 8C.

^{29}Si MAS NMR Spectroscopy. Very recently, a preliminary report on ITQ-1 showed that the as-made material has a large concentration of Si−OH groups due to T−O−T connectivity defects and that most of them are annealed during calcination.[2] Furthermore, defects in the as-made material are not randomly distributed but are predominantly specific of certain crystallographic Si sites. These results came from an ITQ-1 sample synthesized using $TMAda^+$ as the only organic additive and are confirmed in the present work by the study of a much better crystallized ITQ-1 sample synthesized in the presence of $TMAda^+$, HMI, and Na^+.

The ^{29}Si MAS NMR spectrum of as-made ITQ-1 synthesized in the presence of $TMAda^+$, HMI, and Na^+ is shown in Figure 9. The most apparent feature reported in ref 2 is also clearly visible in this sample: a very intense Si(3Si,1OH) peak at ca. −94 ppm, characteristic of very high silica ITQ-1 in its as-made form (Figure 9C). Also, the resonance at −115.5 ppm[2] splits into two resonances of approximately equal intensity at −114.7 and −116.7 ppm. The total concentration of Si−OH connectivity defects here (33%) is about the same as in ref 2 (29.2%). However, calcination at 580 °C produces annealing of these defects, and the ^{29}Si MAS NMR spectrum of the calcined material (Figure 9A) shows no detectable Q^3 species (6.9% residual defects were reported in ref 2). The spectrum of the calcined material shows a much better resolution of Si(4Si) sites than that previously reported (synthesized using only $TMAda^+$),[2] and a significant change of relative intensities is also apparent. Now, seven rather than five Si(4Si) sites are evident. Simulation of the ^{29}Si NMR spectrum of ITQ-1 using the Si−O−Si angles obtained by Rietveld refinement in the present work and the equation of Thomas et al.[18] compares remarkably well with the deconvoluted components of the actual spectrum (Figure 9B,A): there are five resonances with roughly the same intensities and another two (three in the actual structure) with lower intensity. The chemical shifts expand over a very similar range in both the measured and simulated spectra. This comparison allows a tentative assignment of several individual resonances to distinct crystallographic sites, and as seen in Table 6, the assignment proposed previously[2] must be partly revised. The resonance of one of the sites of lower multiplicity (Si1, Si4, or Si5) overlaps with another resonance, preventing a definitive assignment of these sites. Nonetheless, at least two of these sites resonate in the −111.5 to −113 ppm range.

TABLE 6: Assignment of ^{29}Si MAS NMR Resonances for As-Made and Calcined Pure Silica ITQ-1 Synthesized with $TMAda^+$, HMI, and Na^+[a]

as-made ITQ-1			calcined ITQ-1		
δ	I	assignment	δ	I	assignment
−92.6	8.7	Q^2			
−94.1	13.7	Q^3			
−103.7	1.4	Q^3			
−105.0	2.0	Q^4	−105.9	10.9	Q^4, Si2
−108.3	1.2	Q^4	−111.2	10.9	Q^4, Si3
−110.1	20.1	Q^4	−111.8	3.5	Q^4
−112.4	1.8	Q^4	−112.6	5.5	Q^4
−114.7	7.7	Q^4	−113.9	13.7	Q^4, Si8
−116.7	7.3	Q^4	−116.5	13.6	Q^4, Si7
−119.8	8.3	Q^4	−120.3	14.0	Q^4, Si6

[a] Chemical shifts (δ) in ppm from TMS; relative intensities (I) normalized to account for 72 Si atoms per unit cell; for Si site numbering see text and Table 4; Q^n= $Si(OSi)_n(OH)_{(4-n)}$.

The earlier conclusion that the distribution of defects in as-made ITQ-1[2] is not random is confirmed here for the sample synthesized with $TMAda^+$, HMI, and Na^+. The large peak at −94 ppm, assigned to Si(3Si,1OH), and the virtual absence of the resonances at about −106 ppm (characteristic of calcined ITQ-1) and at ca. −114 ppm in as-made ITQ-1 suggest that sites Si2 and Si3 are almost completely Si(3Si,1OH) sites in the precursor. That is, they are only 3-connected. According to the topology of calcined ITQ-1, every site Si2 is connected to two Si3 sites and to sites Si1 and Si4. Thus, we propose that the large concentration of Si−OH defects arises primarily from a specific lack of connectivity between sites Si2 and Si3 and that this is due to the small Si(2)−O(3)−Si(3) angle of 139.8°. It is important to note here that this angle is not imposed by the relatively high symmetry used during the refinement, as O(3) lies on a general position (24r in Wyckoff notation). For all the other Si−O−Si angles the O atom (except O(9)) lies on a high-symmetry site (see Table 4), and these angles are probably biased in the refinement by the choice of a high-symmetry space group. They are very large (180° in Si(1)−

O(1)−Si(1) and Si(4)−O(5)−Si(5)) or very small (136.6° in Si(8)−O(13)−Si(8)). We note that the specific lack of connectivity occurs between the Si sites resonating at a lower field in the ^{29}Si MAS NMR spectrum, i.e., the sites with the smallest average Si−O−Si angles. Moreover, the actual average angle for Si(2) is probably ca. 3° smaller than found in the refinement, as in the actual spectrum it resonates almost 2 ppm at a lower field than in the simulated one. This difference is probably due to the use of constraints during the refinement. Thus, our physical interpretation of the nonrandom distribution of defects is that sites Si2 and Si3, which are relatively strained in the calcined material due to the small Si−O−Si angles, are relaxed in the as-made material by virtue of a systematic lack of connectivity. However, this nonrandom distribution of defects could also be related to the location of the organic molecules, and a structure determination of the as-made material is currently under way to shed more light on this possibility.

Finally, in addition to this interruption of connectivity, it is also possible that a systematic lack of connectivity between adjacent Si1 sites also holds for the pure silica phase if the proposed mechanism for the formation of the final 3-D framework of MCM-22 from the layered precursor14 is correct. Unfortunately, we were unable to assign a single ^{29}Si resonance to site Si1 and thus cannot confirm or rule out this possibility.

Conclusions

ITQ-1, the pure silica analogue of MCM-22, SSZ-25, ERB-1, and PSH-3, can be synthesized hydrothermally using TMAda$^+$ in the absence of alkali cations. Addition of HMI together with TMAda$^+$ allows a faster and more reproducible synthesis, making the crystallization feasible also in the presence of Na^+. Other amines such as DPA exert also a similar, though less effective, beneficial effect, while this is not the case for the slightly bulkier DIBA. ^{13}C CPMAS NMR supports the idea of a "cooperative structure-directing effect" of both the alkylammonium ion and the amine through stabilization by pore filling of two types of void spaces. Thus, we propose that TMAda$^+$ stabilizes the large 12 MR cage and HMI (or other amines of suitable size) stabilizes the smaller sinusoidal 10 MR channels. This cooperative stabilization effect explains the improved synthesis results obtained when using both organic additives.

The synthesis procedures reported here produce ITQ-1 phases with enhanced crystallinity, as compared with MCM-22 and SSZ-25. The XRD patterns are better resolved, and both the crystallinity and the resolution of the XRD patterns are improved when Na^+ is used in a synthesis assisted by HMI and TMAda$^+$. Rietveld refinement of the calcined material in space group *P*6/*mmm* confirms the ITQ-1 possesses the topology previously proposed for MCM-22. Most likely, the 180° Si−O−Si angles imposed by the symmetry are not actually linear, as suggested by the residual electron density around the oxygens located on the 3-fold axis. The O1 and O5 oxygens atoms may deviate slightly from the 3-fold axis in a dynamic and random fashion. This would be in contrast to the findings of recent molecular-mechanics calculations,[19] which show that MCM-22 minimizes to *P*6/*m* with linear Si−O−Si angles.

A similar improvement in resolution is also observed in the ^{29}Si MAS NMR spectra. The spectrum of the calcined material shows a high resolution of crystallographic sites, and the agreement with the spectrum simulated using the refined Si−O−Si angles is remarkable. ^{29}Si MAS NMR spectroscopy indicates that there is a high concentration of defects in as-made ITQ-1 and that these defects are annealed by calcination. The defects are not randomly distributed, and we propose they arise predominantly from unconnected Si2−O−Si3 sites, probably due to the small Si−O−Si angle.

Acknowledgment. M.A.C., M.J.D.-C., and A.C. gratefully acknowledge the Spanish DGICYT (MAT 94-0359-C02-01) for financial support and C. Corell for synthesizing the MCM-22 and SSZ-25 samples and one ITQ-1 sample. We also thank T. Wessels for collecting the synchrotron data set, the staff at the Swiss Norwegian Beamline at the ESRF Grenoble for their help with the operation of the beamline, and L. B. McCusker for many helpful discussions.

References and Notes

(1) Leonowicz, M. E.; Lawton, J. A.; Lawton, S. L.; Rubin, M. K. *Science* **1994**, *264*, 1910.
(2) Camblor, M. A.; Corell, C.; Corma, A.; Díaz-Cabañas, M. J.; Nicolopoulos, S.; González-Calbet, J. M.; Vallet-Regí, M. *Chem. Mater.* **1996**, *8*, 2415.
(3) Corma, A.; Corell, C.; Pérez-Pariente, J. *Zeolites* **1995**, *15*, 2.
(4) Zones, S. I. Eur. Pat. 231860, 1987.
(5) Bennett, J. M.; Chang, C. D.; Lawton, S. L.; Leonowicz, M. E.; Lissy, D. N.; Rubin, M. K. PCT Wo 92/22498, 1992.
(6) Gittleman, C. S.; Bell, A. T.; Radke, C. J. *Catal. Lett.* **1996**, *38*, 1.
(7) Zones, S. I.; Van Nordstrand, R. A.; Santilli, D. S.; Wilson, D. M.; Yuen, L.; Scampavia, L. D. *Stud. Surf. Sci. Catal.* **1989**, *49A*, 299.
(8) Díaz-Cabañas, M. J.; Camblor, M. A.; Corell, C.; Corma, A. Spanish Pat. P9501553, 1995.
(9) Puppe, L.; Weisser, J. US Pat. 4439409, 1984.
(10) Rubin, M. K.; Chu, P. US Pat. 4954325, 1990.
(11) Bellussi, G.; Perego, G.; Clerici, M. G.; Giusti, A. Eur. Pat. Appl., 293032, 1988.
(12) Chan, I. Y.; Labun, P. A.; Pan, M.; Zones, S. I. *Microporous Mater.* **1995**, *3*, 409.
(13) Díaz-Cabañas, M. J.; Camblor, M. A.; Corell, C.; Corma, A. Spanish Pat. P9502306, 1995.
(14) Lawton, S. L.; Jung, A. S.; Kennedy, G. J.; Alemany, L. B.; Chang, C. D.; Hatzikos, G. H.; Lissy, D. N.; Rubin, M. K.; Timken, H. K. C.; Steuernagel, S.; Woessner, D. E. *J. Phys. Chem.* **1996**, *100*, 3788.
(15) Van Nordstrand, R. A.; Santilli, D. S.; Zones, S. I. *ACS Symp. Ser.* **1988**, *368*, 236.
(16) Camblor, M. A.; Yoshikawa, M.; Zones, S. I.; Davis, M. E. *Synthesis of Porous Materials*; Occelli, M., Kessler, H., Eds.; Marcel Dekker: New York, 1997; p 243.
(17) Baerlocher, Ch. X-ray Rietveld System XRS-82, Lab. of Crystallography, ETH, Zurich, Switzerland, 1982.
(18) Thomas, J. M.; Klinowski, J.; Ramdas, S.; Hunter, B. K.; Tenakoon, D. T. B. *Chem. Phys. Lett.* **1983**, *102*, 158.
(19) Njo, S. L.; van Koningsveld, H.; van de Graaf, B. *Chem. Commun.* **1997**, 1243.